Astron. Astrophys. 320, L17–L20 (1997)

ASTRONOMY AND ASTROPHYSICS

LETTER

Letter to the Editor

Millimeter interferometry towards the ultra–compact H II region W3(OH)

F. Wyrowski[1], **P. Hofner**[2], **P. Schilke**[1], **C.M. Walmsley**[1,3], **D.J. Wilner**[4], **and J.E. Wink**[5]

[1] I. Physikalisches Institut, Univ. zu Köln, Zülpicherstr. 77, D-50937 Köln. Germany
[2] Cornell University, NAIC, Arecibo Observatory, P.O. Box 995, Arecibo, P.R. 00613
[3] Osservatorio Astrofisico di Arcetri, Largo E.Fermi 5, I-50125 Firenze, Italy
[4] Harvard Smithsonian Center for Astrophysics , 60 Garden St., Cambridge, MA 02138, USA
[5] Insitut de Radioastronomie Millimétrique, Domaine Universitaire, F-38406 St-Martin-d'Hères, France

Received 10 January 1997 / Accepted 6 Februaray 1997

Abstract. We used the IRAM Interferometer to map the J=1–0 and J=2–1 lines of $C^{17}O$ as well as the continuum at 112 and 225 GHz of the W3(OH) region. Towards the cluster of water masers W3(H_2O) we observed compact continuum emission at both frequencies with spectral index of 3.6 from hot dust emission. The $C^{17}O$ maps show more extended gas with the most massive molecular clump towards W3(H_2O) and none towards W3(OH) itself. We derive a peak column density of 5×10^{23} cm^{-2} at the H_2O maser position. Dust and line fluxes are both consistent with a mass of 10 $M_{\odot}$. Peaks of molecular line channel maps of $C^{17}O$, CH_3OH, and C_2H_5CN show an E–W orientation similar to the cluster of H_2O masers.

Key words: ISM: individual objects: W3(OH) – ISM: clouds – ISM: molecules – radio lines: ISM – Radio continuum: ISM – Techniques: interferometric

1. Introduction

Millimeter interferometers allow us to obtain reliable determinations of the cloud structure in star formation regions and hence the mass distribution. Both millimeter wavelength dust emission and the emission in optically thin isotopomers of CO are thought to trace the H_2 distribution and therefore the mass. One approach is to observe both tracers in a given object and to compare the results. This is best done at a wavelength of 1 mm where dust emission is optically thin but readily observable and where one can observe the (2–1) transitions of e.g. $C^{17}O$ at similar frequencies.

The W3(H_2O) source at a distance of 2.2 kpc (Humphreys 1978) is a warm, high density clump (Turner & Welch 1984) or "hot core" associated with water masers 6″ (0.06 pc) east of the ultra-compact HII region (or UC HII) W3(OH). The strong methanol and OH masers in this direction (Menten et al. 1988) are associated with the ionized gas whereas the H_2O masers appear to be embedded in W3(H_2O) to the east. The water masers appear to be part of a bipolar flow which is also seen in synchrotron radiation at centimeter wavelengths (Reid et al. 1995). Wink et al. (1994) used the IRAM Interferometer to study the W3(H_2O) hot core and detected a continuum source at the molecular line peak which they attributed to emission from hot dust. They estimated a temperature of 100 K for the gas from their methyl cyanide observations and used this to determine a gas mass of 30 $M_{\odot}$. Observations by Wilner et al. (1995) with the BIMA array at 88 GHz confirmed the interpretation of the continuum emission as being due to dust and allowed an improved mass estimate of 10–20 $M_{\odot}$. A single dish molecular line study by Helmich et al. (1994) concluded that the temperature of the molecular gas was likely to be 220 K. These characteristics taken together suggest that the W3(H_2O) hot core is rather similar in character to the well known hot core in Orion (Churchwell 1991 and Walmsley & Schilke 1992).

In this paper, we present new observations of the W3(H_2O) hot core using the IRAM Interferometer at 2.6 and 1.3 mm with resolutions of 3″ and 1.5″, respectively. We imaged the region around the water masers in $C^{17}O$ (1–0) and (2–1) as well as in the dust continuum. Our measurements show the observed emission is indeed due to hot dust and allow an estimate of the dust opacity spectral index. They also allow us to compare mass estimates from $C^{17}O$ and continuum emission.

2. Observations and Data reduction

The observations were carried out in winter 1995/1996 with the IRAM 4-element Array on the Plateau de Bure (Guilloteau

Send offprint requests to: F.Wyrowski

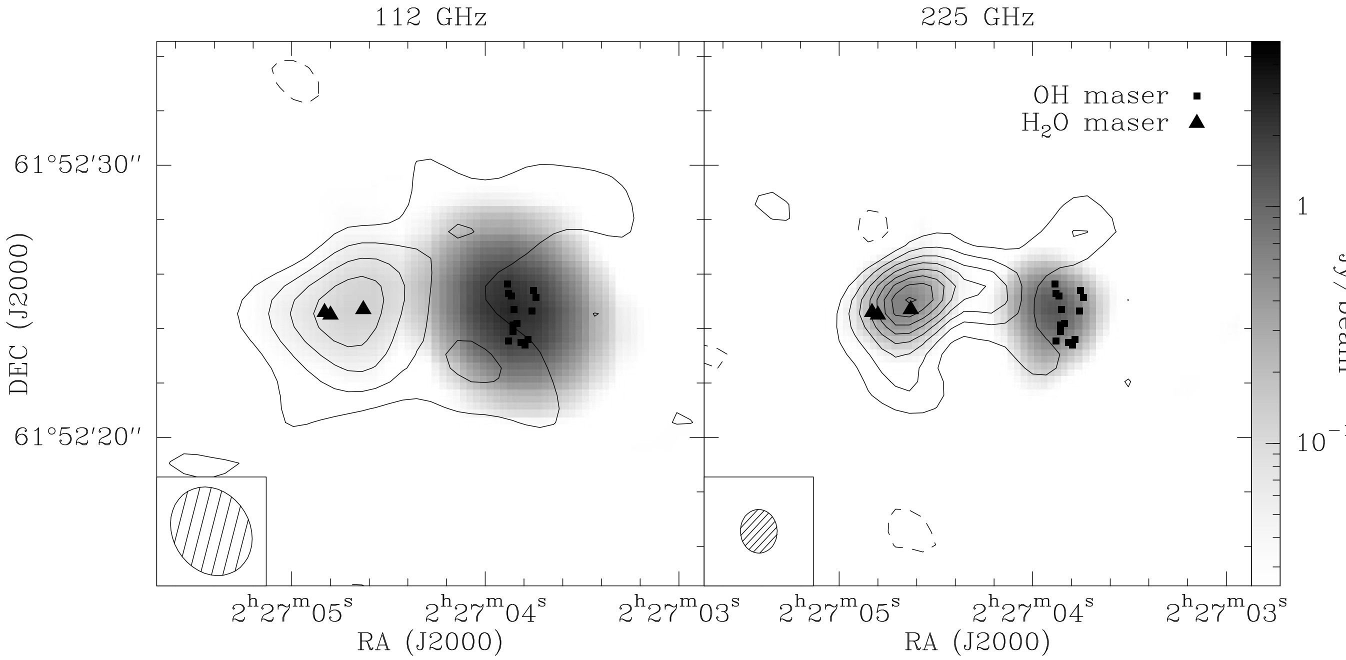

Fig. 1. $C^{17}O$(1–0) integrated emission (left panel, contours) and $C^{17}O$(2–1) (right panel,contours) from the W3(OH) region compared with continuum emission (grey logarithmic scale). Contour steps are 3 and 5.6 Kkm s^{-1} for (1–0) and (2–1), respectively. The positions of the OH masers are from Reid et al. (1980) and the positions of the H_2O masers from Dreher & Welch (1981).

et al. 1992). The primary beam of the 15-m antennas is 45″ at 112 GHz and 22″ at 225 GHz. The synthesized beam was 3.4 × 2.8″ at 112 GHz and 1.6 × 1.4″ at 225 GHz. We were insensitive to structures larger than 17″ at 112 GHz and 6.5″ at 225 GHz. The phase center used for these observation was ($\alpha(J2000)$ = $02^h27^m04\overset{s}{.}284$, $\delta(J2000)$ = 61°52′24.″55) and offsets in this paper are given relative to this position. Our observations of W3(OH) were interspersed at 20 minute intervals with observations of the calibrator 0224+671 for which we used fluxes of 1.1 Jy at 112 GHz and 0.52 Jy at 225 GHz. These fluxes were derived from comparison with NRAO 530 (10.9 Jy at 112 GHz and 7.0 Jy at 225 GHz on Mar 30 1996) and 3C454.3 (4.5 Jy at 112 GHz on Dec 21 1995).

We observed simultaneously at 2.6 and 1.3 mm using SIS receivers with noise temperatures of 40 and 60 K, respectively. The correlator was split so that two units of bandwidth 40 and 80 MHz were centered at the frequencies of $C^{17}O$(1–0) and (2–1) (112358.988 MHz and 224714.368 MHz respectively). The remaining units of bandwidth 160 MHz were blue- and red-shifted 100 MHz to sample the 3 mm and 1.3 mm continuum. These latter frequencies were chosen to be "line free" but some lines were nevertheless detected in these frequency ranges (see below). Velocity resolutions were 0.4 km s^{-1} for $C^{17}O$(1–0), 0.8 km s^{-1} for $C^{17}O$(2–1), 6.7 km s^{-1} in the units used for 3 mm continuum, and 3.3 km s^{-1} in the units used for 1.3 mm continuum.

Continuum maps were constructed using "line free" frequency ranges. At both observing frequencies, the strong ultracompact HII region W3(OH) is clearly visible and this fact allowed us to apply a process of iterative phase-only "self-calibration" to the continuum maps . In order to produce line maps in $C^{17}O$(1-0) and (2-1) and in the other transitions detected, the continuum was subtracted from the line data in the uv-plane.

3. Results

Figure 1 shows our continuum maps at 112 and 225 GHz in greyscale. The r.m.s. noise in these maps is 10 mJy/beam at both frequencies after self-calibration. The 112.5 GHz map is dominated by the UC HII region for which we derive an integrated flux of 3.3 Jy as in earlier determinations (Wink et al. 1994, Wilner et al. 1995). We also detect the continuum source close to the center of expansion of the water masers at an offset of (6.0″, 0.2″) from W3(OH) with a flux of 100 mJy after subtracting a weak positive halo introduced by contamination from W3(OH) due to residual phase errors . This is consistent with the results of Wink et al. (1994). At 225 GHz this source is detected with angular size 2.2 × 1.8″. It is apparently marginally resolved, in contrast to the 88 GHz observation of Wilner which yielded an upper limit of 0.5″. The integrated flux is 1.3 Jy at an offset of (5.5″, 0.2″) from W3(OH). One should note that on scales smaller than our beam, W3(OH) is resolved into a clumpy shell-like structure (Dreher & Welch 1981). Therefore, a centroid is not well defined and this can result in discrepancies of several tenths of an arc second in determining positions relative to W3(OH). The measured flux of W3(OH) at 1.3 mm is 2.6 Jy. This is 20% lower than the extrapolated 3 mm free-free flux which gives the order of the error in determining the fluxes. Reuter et al. (priv. comm.) measured a continuum flux of

6.3 Jy/beam with the IRAM 30-m telescope at 225 GHz in excess of our combined flux of both, W3(OH) and the W3(H_2O), indicating missing flux by the interferometer due to extended emission.

Superimposed on the continuum maps, we show in Fig. 1 our integrated intensity maps in $C^{17}O$. As in the case of $C^{18}O$ (Wink et al. 1994), the $C^{17}O$ emission seen with the interferometer is concentrated on the water maser complex. The continuum emission coincides with the maximum in $C^{17}O$. The J=2–1 emission has a compact core with a half–power size of $4.7 \times 2.7''$ at p.a. 70°, which is more extended than the continuum. There is also , in both the (1–0) and (2–1) transitions, a weak tongue of emission in $C^{17}O$ which wraps around the UC HII region.

In addition to $C^{17}O$, we also detected in the upper sideband the $16_{9,8} - 15_{9,7}$ transition of methanol at 227814.50 MHz (Anderson et al. 1992) and the $25_{3,22} - 24_{3,21}$ transition of ethyl cyanide at 227780.968 MHz. These two transitions have lower level excitation energies of 316.3 and 139.92 K respectively and are thus expected to be emitted in dense hot environments. It is thus not surprising that these lines are compact ($1''$ deconvolved) and coincide with the water maser source. In Fig. 2, we show the positions of maximum emission in $C^{17}O$, C_2H_5CN, and in CH_3OH derived from channel maps in all three lines.

The interesting point which emerges from Fig. 2 is that the peak positions from channel maps towards the water maser source (left panel) are distributed in a structure which is elongated E–W. Similar behavior was seen in methyl cyanide by Wink et al. (1994, their Fig. 9). The shape and size of this structure are similar to the orientation and spatial extent of the water masers mapped by Alcolea et al. (1992) in a VLBI proper motions study. The latter are thought to be in a bipolar flow with an expansion velocity of 20 km s^{-1}. The fact that all of these different tracers have the same orientation suggests that the high excitation molecules trace the sides of the cavity carved out by the outflow. Moreover, the fact that $C^{17}O$(2–1) (a low excitation transition) has a similar spatial distribution suggests that on arc second size scales, the bulk of the mass is in the high temperature gas traced by C_2H_5CN and CH_3OH. Towards this structure, red–shifted velocities are to the west and blue–shifted to the east. However, the water maser data show no very clear blue–red E–W asymmetry. Another scenario is that the hot core gas seen in CH_3OH and C_2H_5CN is in a disk seen edge–on and that the wind is interacting with the surface of this disk and thus giving rise to the water masers. Also a double source cannot be excluded, where the components are associated with the two cm continuum sources seen by Reid et al. (1995) and have different velocities.

4. Mass estimates

Our measurement of the continuum emission at 3 and 1.3 mm allows for the first time a reliable estimate of the dust opacity spectral index at millimeter wavelengths. In Fig. 3, we show the radio continuum spectrum of W3(H_2O) including our new high frequency measurement. At wavelengths longward of 1 cm (Reid et al 1995), synchrotron emission from the jet associated

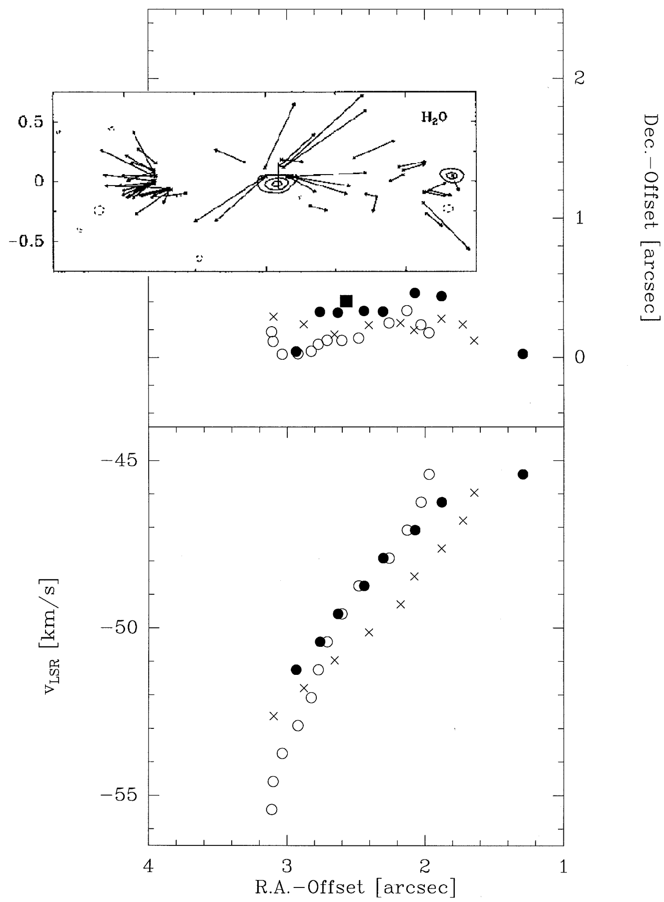

Fig. 2. Peak positions measured in different channels for $C^{17}O$(2–1) (filled circles), A-CH_3OH $16_{9,8} - 15_{9,7}$ (empty circles), and C_2H_5CN $25_{3,22} - 24_{3,21}$ (crosses) towards W3(H_2O) with a synthesized beam size of $1.6 \times 1.4''$. The 225 GHz continuum position is denoted by a filled square. The inset on the left panel shows the water maser proper motion vectors from Alcolea et al. (1992) together with the 15 GHz map of Reid et al. (1995).

with the bipolar molecular outflow is dominant. Between 85 and 225 GHz in contrast, the spectral index is approximately 3.6 and dust emission dominates. The simplest interpretation is that the dust is optically thin with opacity varying as $\nu^{1.6}$.

Knowledge of the opacity index allows us to refine our estimate of the hot core mass. Using an opacity index β of 1.6, we derive (see Wilner et al. 1995) a mass of $23/T_2$ $M_\odot$ where T_2 is the dust temperature in units of 100 K. If one assumes equality of dust and gas temperatures and uses the temperature of 220 K estimated by Helmich et al. (1994), one derives a value of 10 $M_\odot$ for the core seen in continuum emission.

We can also use our $C^{17}O$ results to determine the mass and column density of the molecular gas. The $C^{17}O$(2–1) intensity in a $1.5''$ beam towards W3(H_2O) is 40 Kkm s^{-1} and the ratio of the (2–1) and (1–0) intensities is 1.8 (where we have smoothed to the resolution at 3 mm). This is consistent with emission by hot optically thin gas and one can thus apply canonical formulae (see Genzel 1990) to derive an H_2 column density of 5×10^{23} cm^{-2}. If we integrate this over the observed line emission, we derive

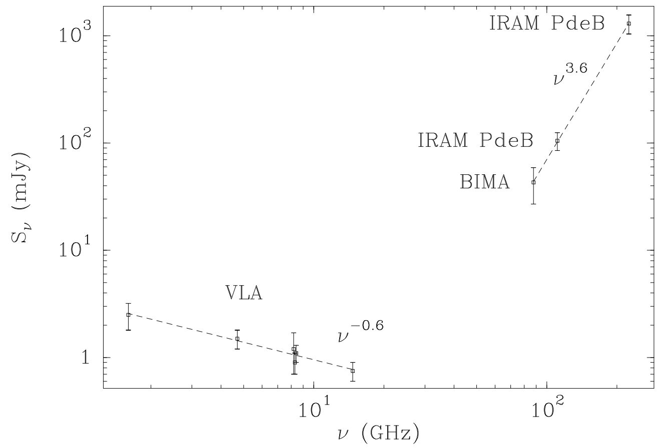

Fig. 3. The radio continuum spectrum of W3(H_2O). At low frequencies, one observes synchrotron emission associated with the outflow (Menten & Reid 1994) and at high frequencies dust emission from the hot core.

a mass of 11 $M_\odot$ or, integrated over the size of the continuum source, of 4 $M_\odot$.

Both of these are considerably less than the upper limit to the "virial mass" (roughly 60 $M_\odot$) which one derives from the observed line widths and the angular size of the gas indicating that the virial assumption is not valid due to the dynamics of the outflow. It is interesting to note that the masses we derive for the hot core gas are comparable to the probable mass of the star which is presumably responsible for the observed high temperatures. Model calculations we have carried out suggest that one requires a central star of luminosity at least 10^4 solar luminosities to account for temperatures of 100 K at radii of 1000 AU. Such a star if on the ZAMS (spectral type B0, see Panagia 1973) should have a mass of roughly 15 $M_\odot$ which is comparable to our estimate for the hot core mass based on the millimeter emission. The rotation velocity at a distance of 1000 AU (0.5″) from such a star (roughly 4 km s^{-1}) is approximately of the order needed to explain the velocity shift with right ascension seen in Fig. 2. This seems consistent with the edge–on disk scenario mentioned above.

5. Conclusions

This study has allowed us to compare mass estimates of different types for the molecular hot core W3(H_2O). Using estimates both from the millimeter dust emission and from optically thin $C^{17}O$, we conclude that the mass of the hot (100-200 K) gas within 1000 AU of the young star responsible for the observed activity is 10 $M_\odot$. This is comparable to the probable mass of the young embedded star. Our data show that the E–W orientation of the channel map peaks and the velocity gradient seen by Wink et al. is a general characteristic of the hot core gas which is either related to the bipolar outflow inferred by water maser proper motions or with a rotating disk. Only higher resolution can resolve this issue.

References

Alcolea J., Menten K.M., Moran J.M., Reid M.J. 1992, in *Astrophysical Masers*, ed. A.W.Clegg and G.E.Nedoluha, publ. Springer (Heidelberg)
Anderson T., Herbst E., De Lucia F. 1992, ApJS, 82, 405
Churchwell E. 1991, in *the Physics of Star Formation and early Stellar Evolution*, NATO Asi, eds. C.J. Lada and N. Kylafis
Dreher J.W., Welch W.J. 1981 ApJ, 245, 857
Genzel R. 1991:"Physics and Chemistry of Molecular Clouds", in *Galactic Interstellar Medium*, ed. W.B. Burton et al. (Springer, Berlin)
Guilloteau S. et al. 1992 A&A, 262, 624
Helmich F.P., Jansen D.J., de Graauw T., Groesbeck T.D., van Dishoeck E.F. 1994 A&A, 283, 626
Humphreys R.H. 1978, ApJS 38, 309
Menten K.M., Reid M.J., Moran J.M., Wilson T.L., Johnston K.J., Batrla W. 1988, ApJ, 333, L83
Panagia N. 1973, AJ, 78, 929
Reid M.J., et al. 1980, ApJ 239, 89
Reid M.J., Argon A.L., Masson C.R., Menten K.M., Moran J.M. 1995, ApJ, 443, 238
Turner J.L., Welch W.J. 1984, ApJ, 287, L81
Walmsley C.M., Schilke P. 1992, in *Dust and Chemistry in Astronomy*, eds. Millar T.J., Williams D.A., IOP Publ.
Wilner D.J., Welch W.J., Forster J.R. 1995 , ApJ, 449, L73
Wink J.E., Duvert G., Guilloteau S., Güsten R., Walmsley C.M., Wilson T.L. 1994, A&A, 281, 505

This article was processed by the author using Springer-Verlag LaTeX A&A style file *L-AA* version 3.